

Hadronic light-by-light contribution to muon $g - 2$ with lattice QCD and infinite volume, continuum QED

TOM BLUM

UConn

NORMAN CHRIST

Columbia

MASASHI HAYAKAWA

Nagoya

TAKU IZUBUCHI

BNL/RBRC

LUCHANG JIN

UConn/RBRC

CHRISTOPH LEHNER

BNL

Jan 08 2018

Jefferson Lab, Newport News, VA

Theory Seminar

- **Introduction**
- Method
- Simulation
- Infinite volume QED box
- Summary



Figure 1. The headstone of Julian Schwinger at Mt Auburn Cemetery in Cambridge, MA.

Accurate Determination of the μ^+ Magnetic Moment*R. L. GARWIN,[†] D. P. HUTCHINSON, S. PENMAN,[‡] AND G. SHAPIRO[§]
Columbia University, New York, New York

(Received August 4, 1959)

Using a precession technique, the magnetic moment of the positive mu meson is determined to an accuracy of 0.007%. Muons are brought to rest in a bromoform target situated in a homogeneous magnetic field, oriented at right angles to the initial muon spin direction. The precession of the spin about the field direction, together with the asymmetric decay of the muon, produces a periodic time variation in the probability distribution of electrons emitted in a fixed laboratory direction. The period of this variation is compared with that of a reference oscillator by means of phase measurements of the "beat note" between the two. The magnetic field at which the precession and reference frequencies coincide is measured with reference to a proton nuclear magnetic resonance magnetometer. The ratio of the muon precession frequency to that of the proton in the same magnetic field is thus determined to be 3.1834 ± 0.0002 . Using a re-evaluated lower limit to the muon mass, this is shown to yield a lower limit on the muon g factor of $2(1.00122 \pm 0.00008)$, in agreement with the predictions of quantum electrodynamics.

I. INTRODUCTION

RECENT developments in the theory of weak interactions¹ make it appear that many of the properties of the mu meson can be accounted for on the assumption that it enters into interactions in the same way as the electron but has a much larger mass. The electromagnetic properties of the muon, therefore, acquire increased interest as a further test of the identity of the interactions of the two particles.

Quantum electrodynamics² makes the prediction that the magnetic moment of a spin-1/2 Dirac particle is

of detecting the direction of polarization via their asymmetric decay⁶ made possible the measurement of the muon magnetic moment. In the original experiment it was found necessary, to obtain agreement with the asymmetry curve, to assume a value of the moment close to the Dirac prediction. In this way the value was determined to an accuracy of 1%. The Liverpool group,⁷ using an analog time-to-height converter to record the distribution in time of the emitted electrons, achieved an accuracy of 0.7%. A resonance technique, in which the muons were stopped in a large static magnetic

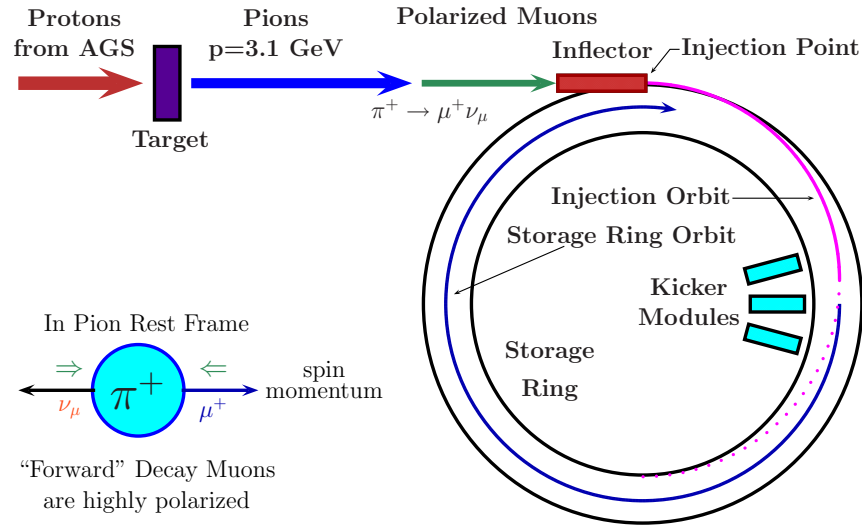


Figure 2. The schematics of muon injection and storage in the $g - 2$ ring. Phys. Rept. **477**, 1 (2009).

$$\omega_c = \frac{eB}{m_\mu \gamma} \tag{1}$$

$$\omega_s = \frac{eB}{m_\mu \gamma} + a_\mu \frac{eB}{m_\mu} \tag{2}$$

$$\gamma = 1/\sqrt{1-v^2} \approx 29.3 \tag{3}$$

Authors	Lab	Muon Anomaly
Garwin et al. '60	CERN	0.001 13(14)
Charpak et al. '61	CERN	0.001 145(22)
Charpak et al. '62	CERN	0.001 162(5)
Farley et al. '66	CERN	0.001 165(3)
Bailey et al. '68	CERN	0.001 166 16(31)
Bailey et al. '79	CERN	0.001 165 923 0(84)
Brown et al. '00	BNL	0.001 165 919 1(59) (μ^+)
Brown et al. '01	BNL	0.001 165 920 2(14)(6) (μ^+)
Bennett et al. '02	BNL	0.001 165 920 4(7)(5) (μ^+)
Bennett et al. '04	BNL	0.001 165 921 4(8)(3) (μ^-)

World Average dominated by BNL

$$a_\mu = (11659208.9 \pm 6.3) \times 10^{-10} \quad (4)$$

In comparison, for electron

$$a_e = (11596521.8073 \pm 0.0028) \times 10^{-10} \quad (5)$$



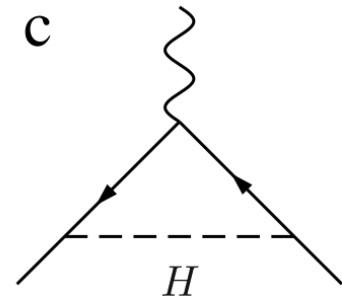
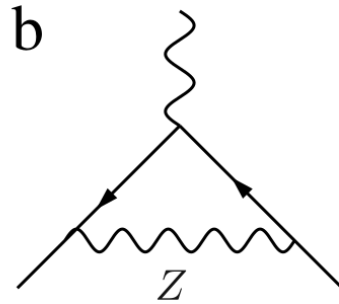
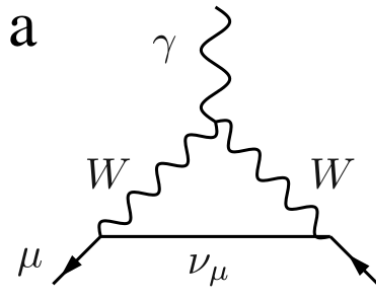
Figure 3. 1000 Piece Jigsaw Puzzle - Magnetic Moment. \$18.00 from <http://eddata.fnal.gov/>

Almost 4 times more accurate than the previous experiment.

J-PARC E34 also plans to measure muon $g - 2$ with similar precision.

$$\begin{aligned}
a_\mu^{\text{QED}} &= 0.5 \times \left(\frac{\alpha}{\pi}\right) + 0.765\,857\,425 \underbrace{(17)}_{m_\mu/m_{e,\tau}} \times \left(\frac{\alpha}{\pi}\right)^2 \\
&\quad + 24.050\,509\,96 \underbrace{(32)}_{m_\mu/m_{e,\tau}} \times \left(\frac{\alpha}{\pi}\right)^3 + 130.8796 \underbrace{(63)}_{\text{num. int.}} \times \left(\frac{\alpha}{\pi}\right)^4 \\
&\quad + 753.29 \underbrace{(1.04)}_{\text{num. int.}} \times \left(\frac{\alpha}{\pi}\right)^5 \\
&= 116\,584\,718.853 \underbrace{(9)}_{m_\mu/m_{e,\tau}} \underbrace{(19)}_{c_4} \underbrace{(7)}_{c_5} \underbrace{(29)}_{\alpha(a_e)} [36] \times 10^{-11}
\end{aligned}$$

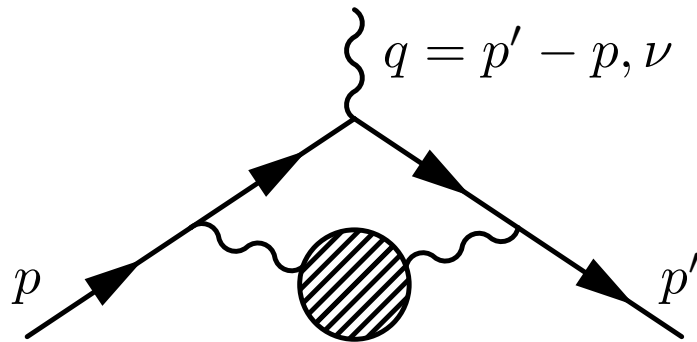
Aoyama et al. '12



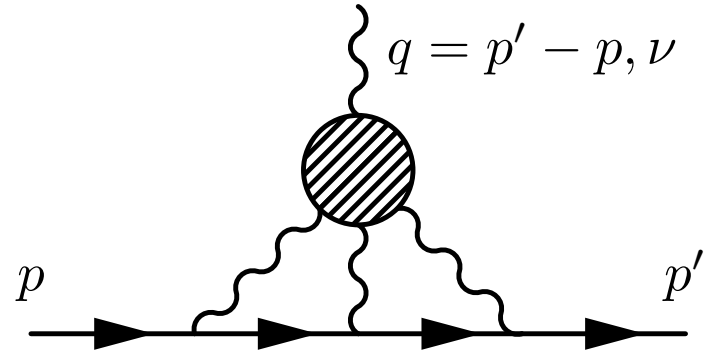
Leading weak contribution. $a = 38.87, b = -19.39, c = 0.00$ [in units 10^{-10}]

	Value \pm Error	Reference
QED incl. 5-loops	11658471.8853 ± 0.0036	Aoyama, et al, 2012
Weak incl. 2-loops	15.36 ± 0.10	Gnendiger et al, 2013

Table 1. Standard model theory, QED and Weak interaction. [in units 10^{-10}]



(L) HVP



(R) HLbL

- HVP: hadronic vacuum polarization.

The following results are obtained with dispersion relations using $e^+e^- \rightarrow \text{hadrons}$ data.

692.3 ± 4.2 , DHMZ10. arXiv:1010.4180

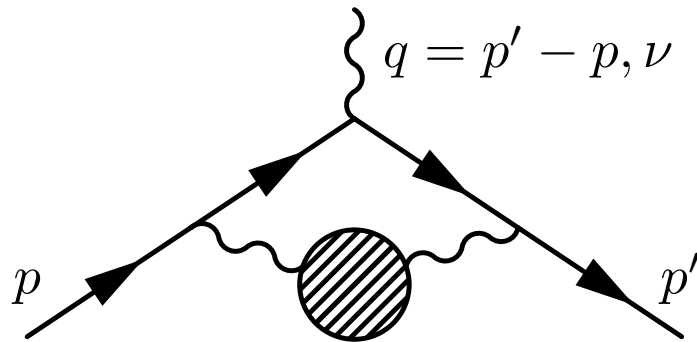
694.9 ± 4.3 , HLMNT11. arXiv:1105.3149

688.1 ± 4.2 , FJ17. arXiv:1705.00263

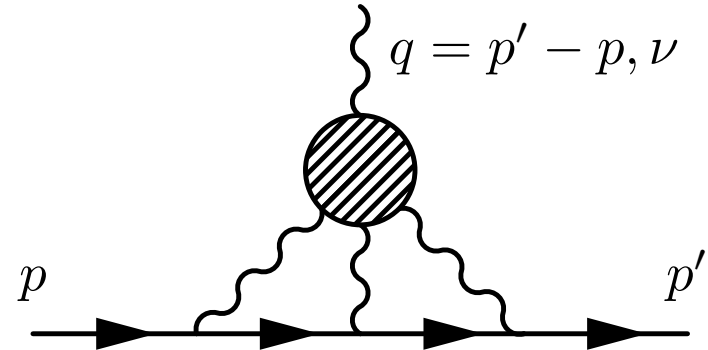
693.1 ± 3.4 , DHMZ17. arXiv:1706.09436

692.2 ± 2.6 , KNT17. Alex Keshavarzi talk given at Fermilab, 3 Jun 2017.

- HVP NLO: -9.84 ± 0.07 , HLMNT11. arXiv:1105.3149



(L) HVP



(R) HLbL

- HLbL: hadronic light-by-light scattering.

The following results are obtained with combinations of models on different process.

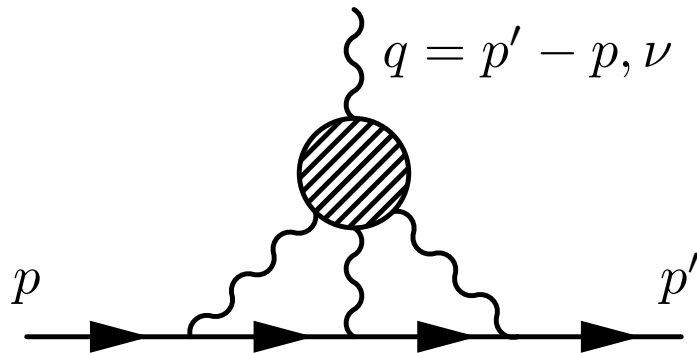
10.5 ± 2.6 PdRV09, Glasgow consensus, arXiv:0901.0306.

10.5 ± 4.9 same as above, but errors added linearly instead of in quadrature.

11.6 ± 3.9 JN09, arXiv:0902.3360.

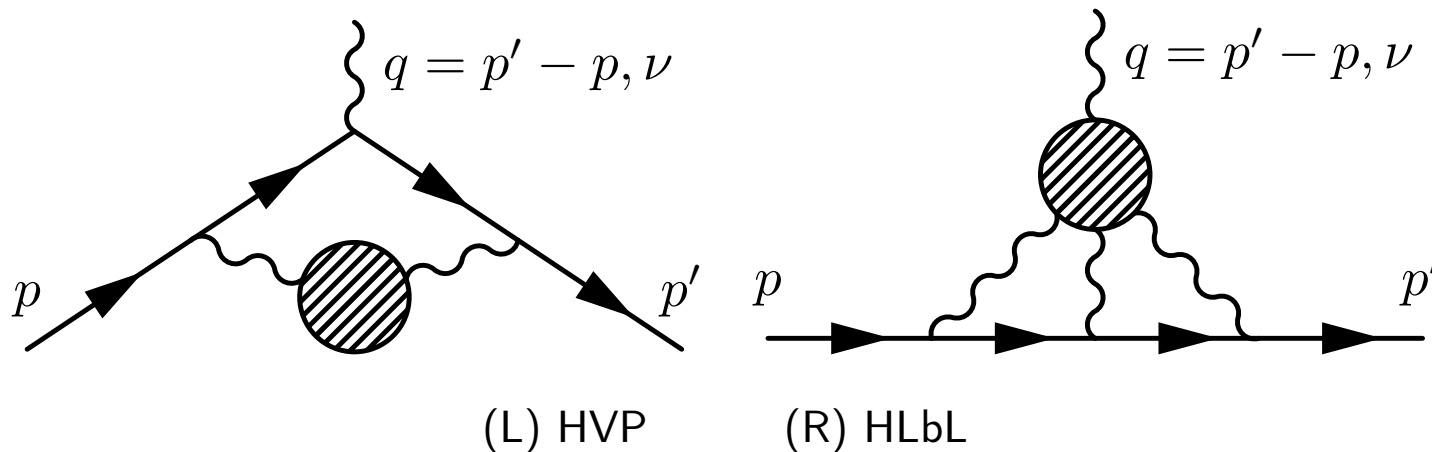
10.3 ± 2.9 FJ17, arXiv:1705.00263.

- Dispersive approach.



Various contributions to $a_{\mu}^{\text{HLbL}} \times 10^{10}$

	PdRV09 (Glasgow consensus)	JN09	FJ17
π^0, η, η'	11.4 ± 1.3	9.9 ± 1.6	9.5 ± 1.2
π, K loops	-1.9 ± 1.9	-1.9 ± 1.3	-2.0 ± 0.5
axial-vector	1.5 ± 1.0	2.2 ± 0.5	0.8 ± 0.3
scalar	-0.7 ± 0.7	-0.7 ± 0.2	-0.6 ± 0.1
quark loops	0.2 (charm)	2.1 ± 0.3	2.2 ± 0.4
tensor	-	-	0.1 ± 0.0
NLO	-	-	0.3 ± 0.2
Total	10.5 ± 4.9	11.6 ± 3.9	10.3 ± 2.9
	10.5 ± 2.6 (quadrature)		



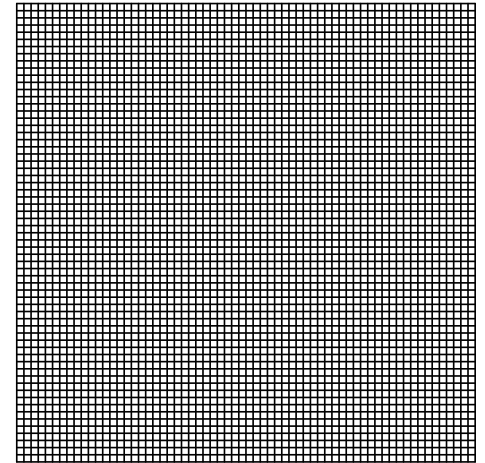
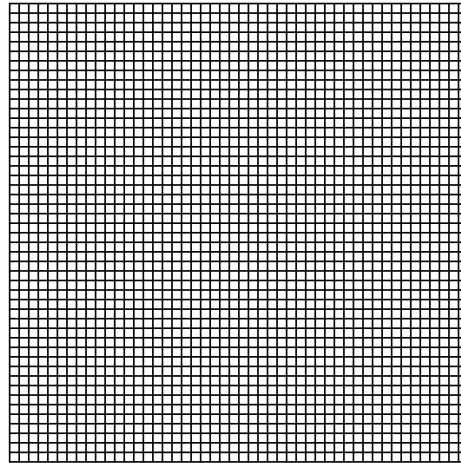
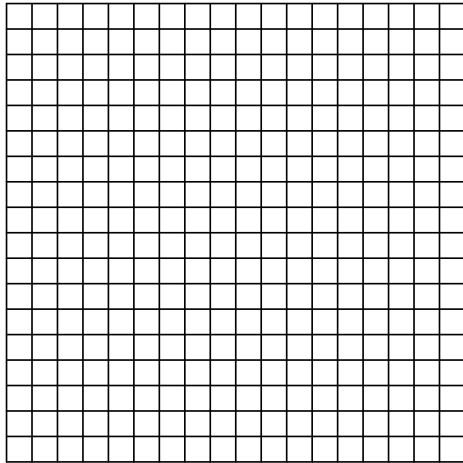
	$a_\mu \times 10^{10}$	
HVP ($e^+e^- \rightarrow \text{hadrons}$)	692.2 ± 2.6	KNT17
Hadronic Light by Light	10.3 ± 2.9	FJ17
Standard Model	11659179.9 ± 3.9	
Experiment (0.54 ppm)	11659208.9 ± 6.3	E821, The $g - 2$ Collab. 2006
Difference (Exp - SM)	29.0 ± 7.4	

Table 2. Standard model theory and experiment comparison

There is 3.9 standard deviations!

The QCD partition function in Euclidean space time:

$$Z = \int [\mathcal{D}U_\mu] e^{-S_G[U]} \det(D[m_l, U])^2 \det(D[m_s, U]) \quad (6)$$



(Left) 19×19 Go board (Middle) 48×48 (Right) 64×64

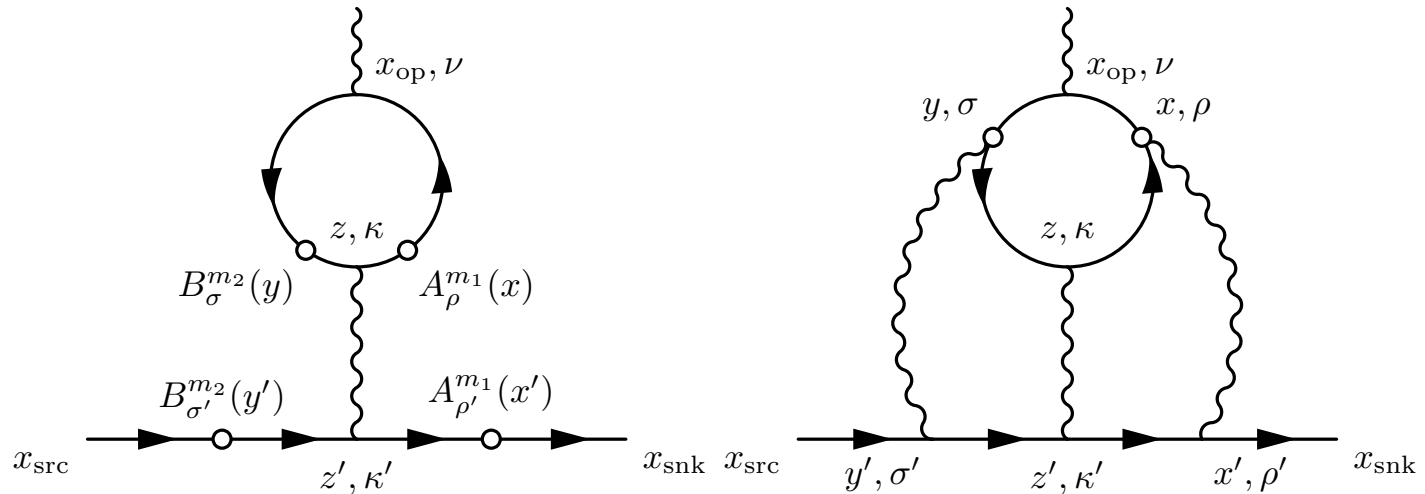
The configuration is stored in position space. The reason is that the action is local in position space. Working in position makes the calculation simpler.

This is in contrast to analytical perturbative calculation, where interaction only happens occasionally. So it is advantageous to work in momentum space, where the propagator can be diagonalized.

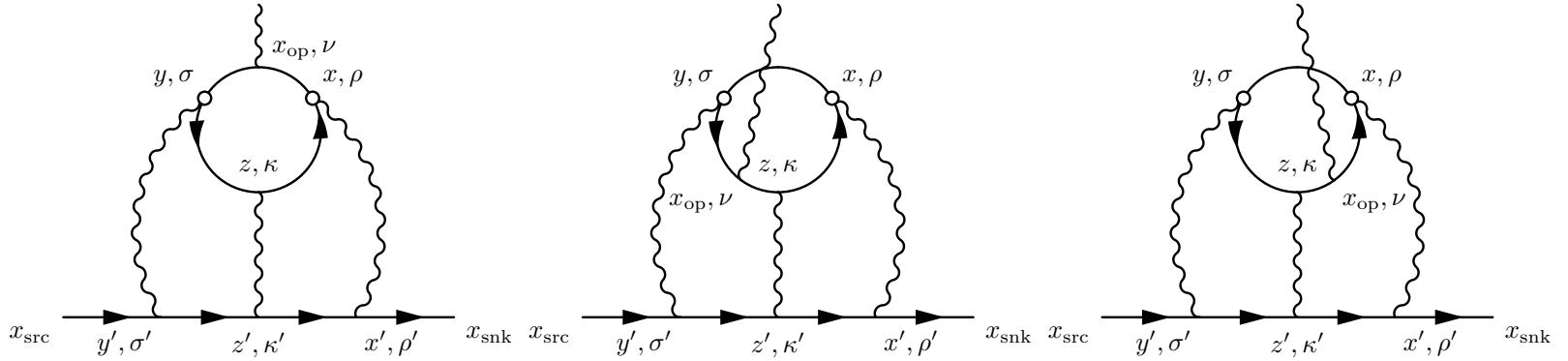
- Introduction
- **Method**
- Simulation
- Infinite volume QED box
- Summary

- This subject is started by T. Blum, S. Chowdhury, M. Hayakawa, T. Izubuchi more than 7 years ago. **hep-lat/0509016, Phys.Rev.Lett. 114 (2015) no.1, 012001.**
- A series of improvements in methodology is made later. We computed the connected diagram of HLbL with 171 MeV pion mass. **Phys.Rev. D93 (2016) no.1, 014503.**
- Mainz group independently come up with a similar method to compute HLbL. **PoS LATTICE2015 (2016) 109.**
- With the improved methods, we calculated HLbL using the physical pion mass, $48^3 \times 96$, ensemble. And for the first time, we computed the leading disconnected diagrams contribution. **Phys.Rev.Lett. 118 (2017) no.2, 022005.**
- Mainz group announces the significant progress on the method to reduce the finite volume effects by treating the QED part of the HLbL diagram semi-analytically in infinite volume. Part of the results are given in **PoS LATTICE2016 (2016) 164.**
- Encouraged by Mainz's success, we use a different approach to compute the QED part of the HLbL in infinite volume. Based the results, we exploit a way to further reduce the lattice discretization error and finite volume error. **Phys.Rev. D96 (2017), 034515.**
- Final goal is reaching 10% accuracy to compare with the new experiments.

RBC's version of the history on this subject.



- Left: the two photon propagators are represented by ensemble average of QED configurations.
- Right: the two photon propagators are represented by random sampling of point source locations.
- Goal: Keep the signal unchanged, reduce the noise as much as possible.



$$\mathcal{F}_\nu^C(\vec{q}; x, y, z, x_{\text{op}}) = (-ie)^6 \mathcal{G}_{\rho, \sigma, \kappa}(\vec{q}; x, y, z) \mathcal{H}_{\rho, \sigma, \kappa, \nu}^C(x, y, z, x_{\text{op}}) \quad (7)$$

$$\begin{aligned} & i^4 \mathcal{H}_{\rho, \sigma, \kappa, \nu}^C(x, y, z, x_{\text{op}}) \quad (8) \\ = & \sum_{q=u, d, s} \frac{(e_q/e)^4}{6} \left\langle \text{tr} \left[-i\gamma_\rho S_q(x, z) i\gamma_\kappa S_q(z, y) i\gamma_\sigma S_q(y, x_{\text{op}}) i\gamma_\nu S_q(x_{\text{op}}, x) \right] \right\rangle_{\text{QCD}} \\ & + \text{other 5 permutations} \end{aligned}$$

$$\begin{aligned} & i^3 \mathcal{G}_{\rho, \sigma, \kappa}(\vec{q}; x, y, z) \quad (9) \\ = & e^{\sqrt{m_\mu^2 + \vec{q}^2/4}(t_{\text{snk}} - t_{\text{src}})} \sum_{x', y', z'} G_{\rho, \rho'}(x, x') G_{\sigma, \sigma'}(y, y') G_{\kappa, \kappa'}(z, z') \\ & \times \sum_{\vec{x}_{\text{snk}}, \vec{x}_{\text{src}}} e^{-i\vec{q}/2 \cdot (\vec{x}_{\text{snk}} + \vec{x}_{\text{src}})} S_\mu(x_{\text{snk}}, x') i\gamma_{\rho'} S_\mu(x', z') i\gamma_{\kappa'} S_\mu(z', y') i\gamma_{\sigma'} S_\mu(y', x_{\text{src}}) \\ & + \text{other 5 permutations} \end{aligned}$$

Classicaly, magnetic moment is simply

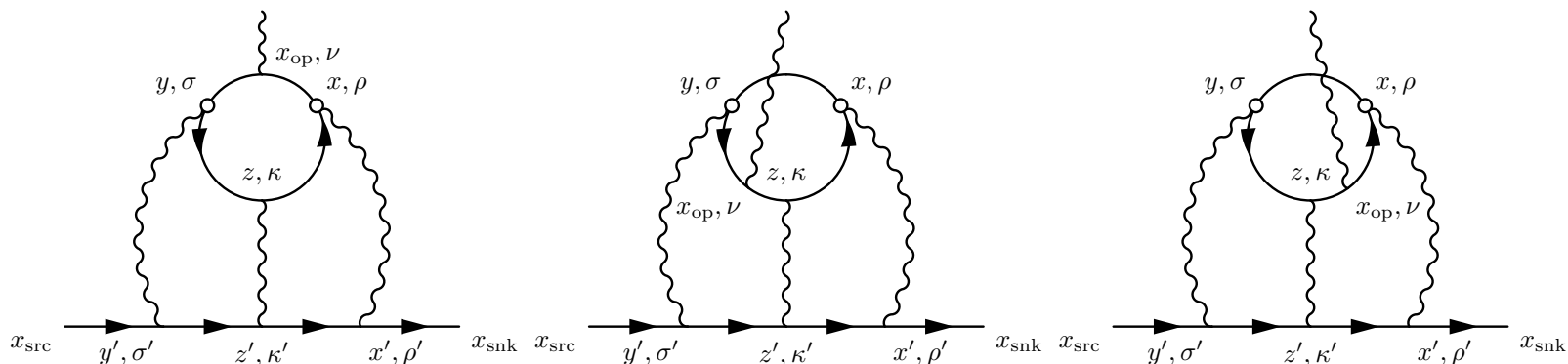
$$\vec{\mu} = \int \frac{1}{2} \vec{x} \times \vec{j} d^3x \quad (10)$$

- This formula is not correct in Quantum Mechanics, because the magnetic moment result from the spin is not included.
- In Quantum Field Thoery, Dirac equation automatically predict fermion spin, so the naive equation is correct again!

$$\langle \vec{\mu} \rangle = \left\langle \psi \left| \int \frac{1}{2} \vec{x}_{\text{op}} \times i \vec{j}(\vec{x}_{\text{op}}) d^3x_{\text{op}} \right| \psi \right\rangle \quad (11)$$

- $i \vec{j}(\vec{x}_{\text{op}})$ is the conventional Minkovski spatial current, because of our γ matrix convention.
- The right hand generate the total magnetic moment for the entire system, including magnetic moment from spin.
- Above formula applies to **normalizable state** with zero total current. Not practical on lattice because it need extremely large volume to evaluate.

$$L \gg \Delta x_{\text{op}} \sim 1 / \Delta p \quad (12)$$



$$\frac{F_2(0)}{m} \bar{u}_{s'}(\vec{0}) \frac{\vec{\Sigma}}{2} u_s(\vec{0}) = \sum_r \left[\sum_{z, x_{\text{op}}} \frac{1}{2} \vec{x}_{\text{op}} \times \bar{u}_{s'}(\vec{0}) i\vec{\mathcal{F}}^C \left(\vec{0}; x = -\frac{r}{2}, y = +\frac{r}{2}, z, x_{\text{op}} \right) u_s(\vec{0}) \right]$$

- The initial and final muon states are plane waves instead of properly normalized states.
- Recall the definition for \mathcal{F}_μ , we sum all the internal points over the entire space time except we fix $x + y = 0$.
- The time coordinate of the current, $(x_{\text{op}})_0$ is integrated instead of being held fixed.

These features allow us to perform the lattice simulation efficiently in finite volume.

- One diagram (the biggest diagram below) do not vanish even in the $SU(3)$ limit.
- We extend the method and computed this leading disconnected diagram as well.

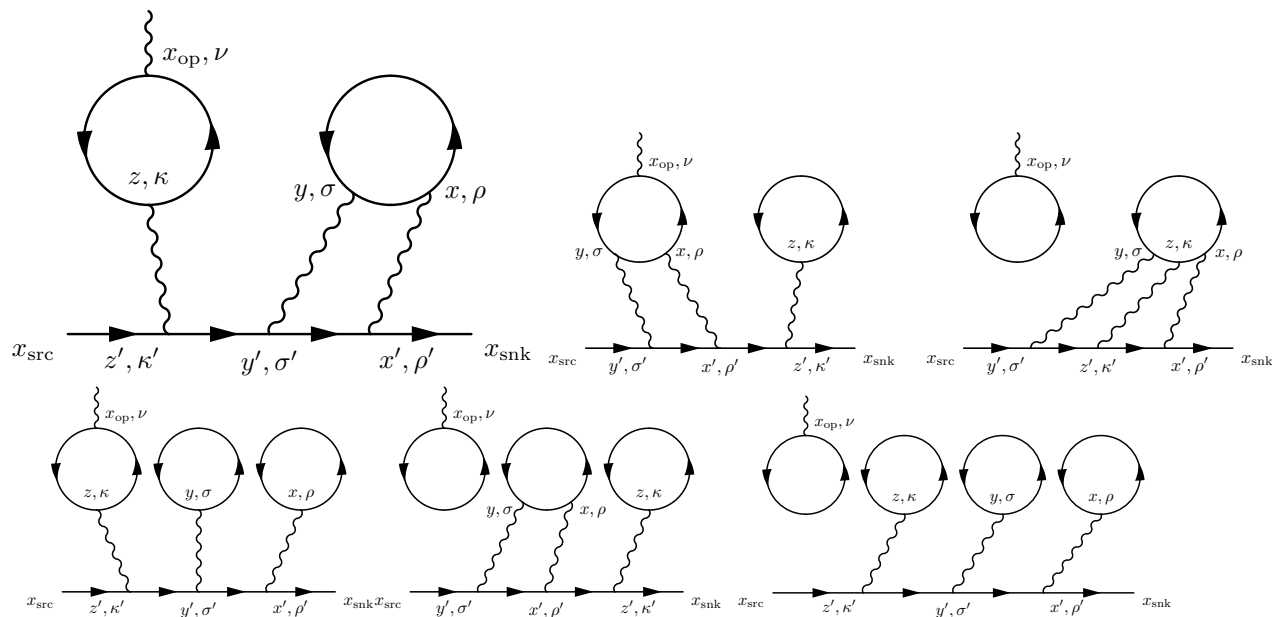
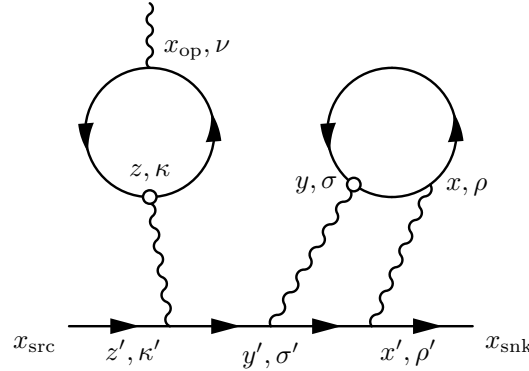


Figure 4. All possible disconnected diagrams. Permutations of the three internal photons are not shown.

- There should be gluons exchange between and within the quark loops, but are not drawn.
- We need to make sure that the loops are connected by gluons by “vacuum” subtraction. So the diagrams are 1-particle irreducible.

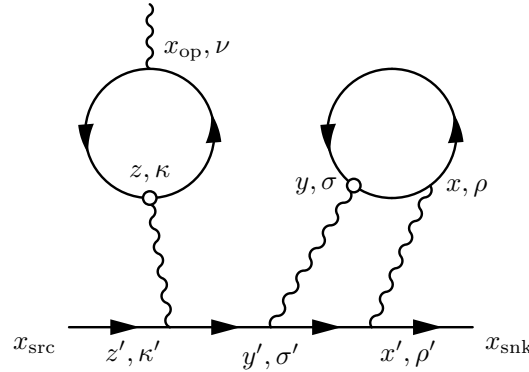


- We can use two point source photons at y and z , which are chosen randomly. The points x_{op} and x are summed over exactly on lattice.
- Only point source quark propagators are needed. We compute M point source propagators and all M^2 combinations of them are used to perform the stochastic sum over $r = z - y$.

$$\mathcal{F}_\nu^D(x, y, z, x_{\text{op}}) = (-ie)^6 \mathcal{G}_{\rho, \sigma, \kappa}(x, y, z) \mathcal{H}_{\rho, \sigma, \kappa, \nu}^D(x, y, z, x_{\text{op}}) \quad (13)$$

$$\mathcal{H}_{\rho, \sigma, \kappa, \nu}^D(x, y, z, x_{\text{op}}) = \left\langle \frac{1}{2} \Pi_{\nu, \kappa}(x_{\text{op}}, z) [\Pi_{\rho, \sigma}(x, y) - \Pi_{\rho, \sigma}^{\text{avg}}(x - y)] \right\rangle_{\text{QCD}} \quad (14)$$

$$\Pi_{\rho, \sigma}(x, y) = - \sum_q (e_q/e)^2 \text{Tr}[\gamma_\rho S_q(x, y) \gamma_\sigma S_q(y, x)]. \quad (15)$$



$$\frac{F_2^{\text{dHLbL}}(0)}{m} \frac{(\sigma_{s'}, s)_i}{2} = \sum_{r, x} \sum_{x_{\text{op}}} \frac{1}{2} \epsilon_{i, j, k} (\tilde{x}_{\text{op}})_j \cdot i \bar{u}_{s'}(\vec{0}) \mathcal{F}_k^D(x, y=r, z=0, x_{\text{op}}) u_s(\vec{0}) \quad (16)$$

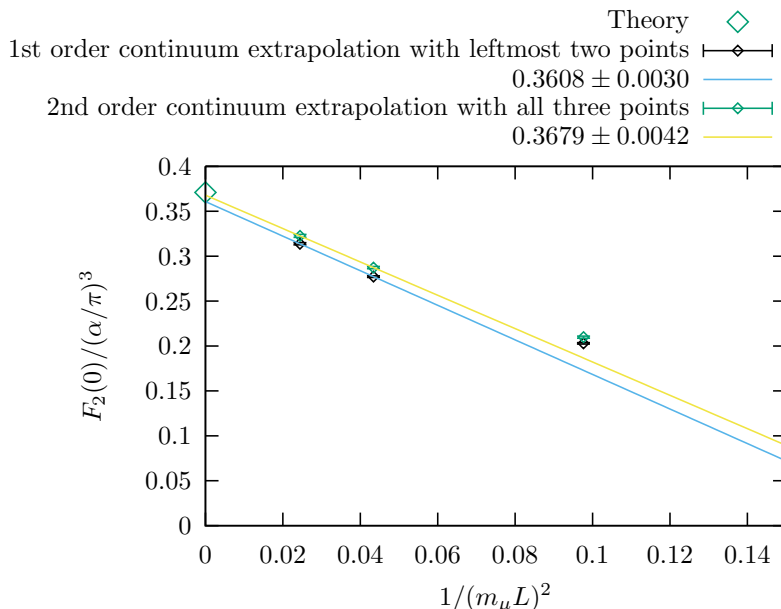
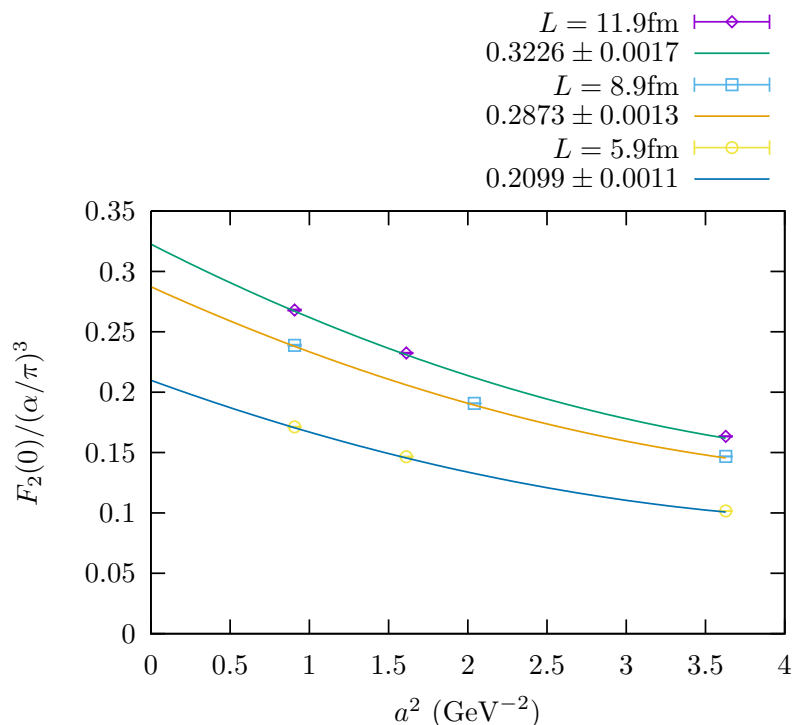
$$\mathcal{H}_{\rho, \sigma, \kappa, \nu}^D(x, y, z, x_{\text{op}}) = \left\langle \frac{1}{2} \Pi_{\nu, \kappa}(x_{\text{op}}, z) [\Pi_{\rho, \sigma}(x, y) - \Pi_{\rho, \sigma}^{\text{avg}}(x - y)] \right\rangle_{\text{QCD}} \quad (17)$$

$$\sum_{x_{\text{op}}} \frac{1}{2} \epsilon_{i, j, k}(x_{\text{op}})_j \langle \Pi_{\rho, \sigma}(x_{\text{op}}, 0) \rangle_{\text{QCD}} = \sum_{x_{\text{op}}} \frac{1}{2} \epsilon_{i, j, k}(-x_{\text{op}})_j \langle \Pi_{\rho, \sigma}(-x_{\text{op}}, 0) \rangle_{\text{QCD}} = 0$$

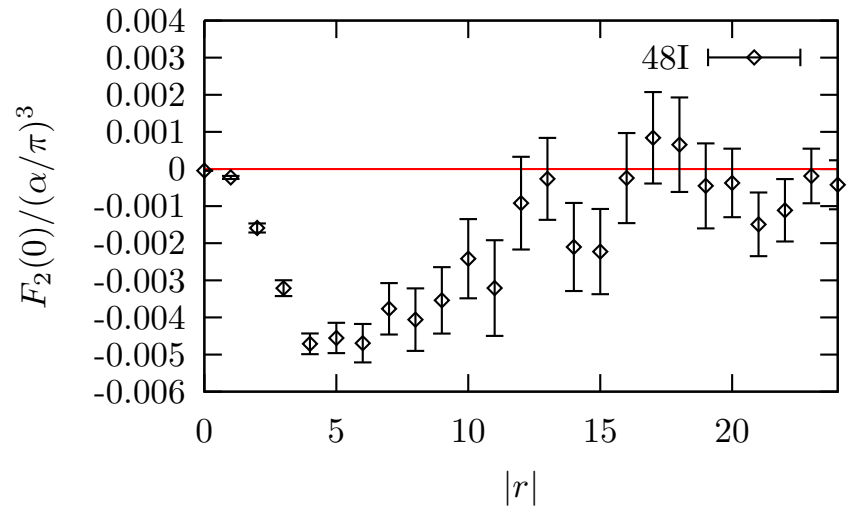
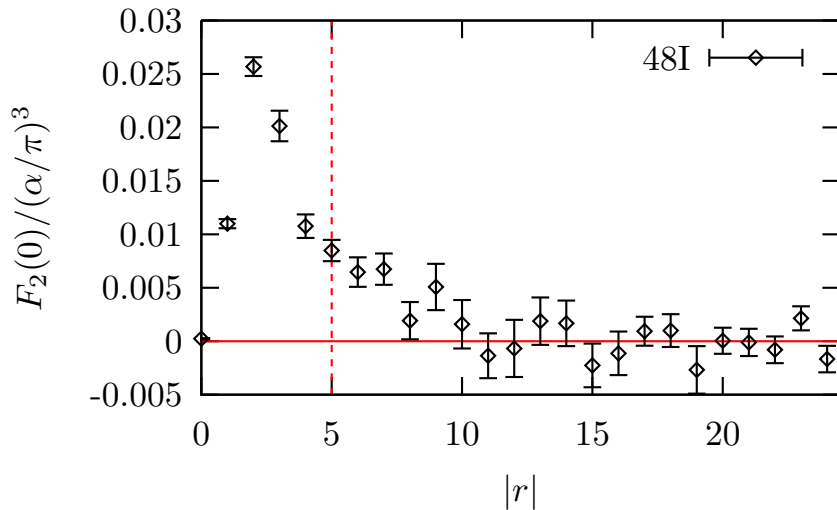
- Because of the parity symmetry, the expectation value for the left loop average to zero.
- $[\Pi_{\rho, \sigma}(x, y) - \Pi_{\rho, \sigma}^{\text{avg}}(x - y)]$ is only a noise reduction technique. $\Pi_{\rho, \sigma}^{\text{avg}}(x - y)$ should remain constant through out the entire calculation.

- Introduction
- Method
- **Simulation**
- Infinite volume QED box
- Summary

- We test our setup by computing **muon leptonic light by light** contribution to muon $g - 2$.



- Pure QED computation.** Muon leptonic light by light contribution to muon $g - 2$. Phys.Rev. D93 (2016) 1, 014503. arXiv:1510.07100.
- $\mathcal{O}(1/L^2)$ finite volume effect, because the photons are emitted from a conserved loop.



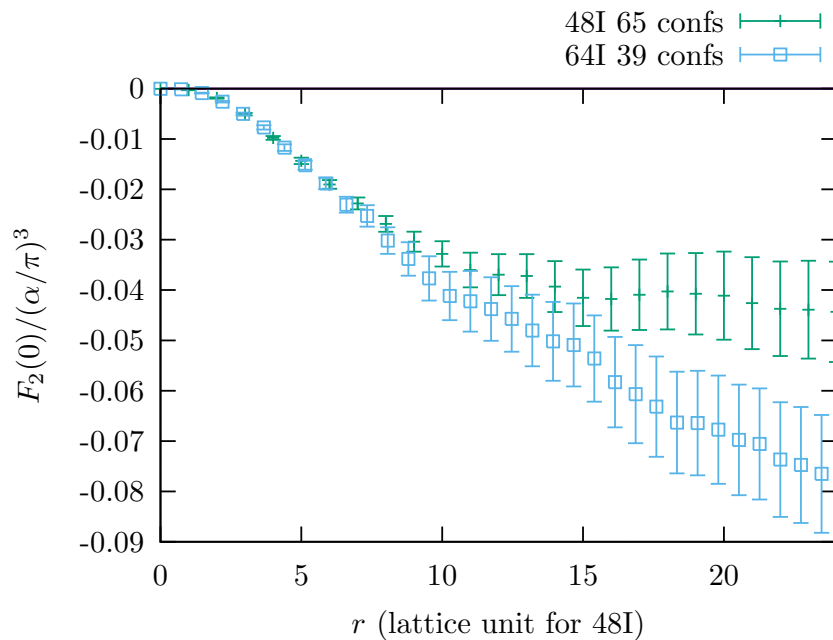
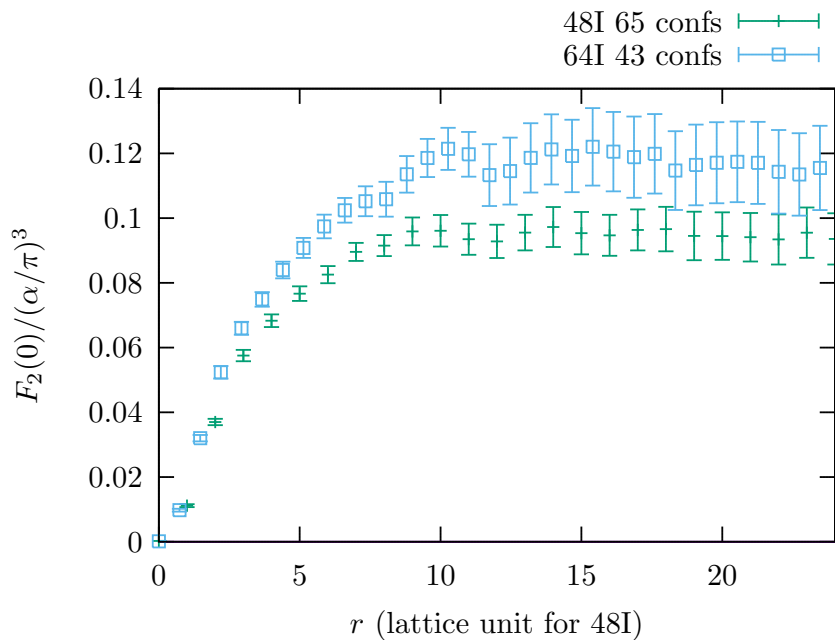
- Left: connected diagrams contribution. Right: leading disconnected diagrams contribution.
- $48^3 \times 96$ lattice, with $a^{-1} = 1.73$ GeV, $m_\pi = 139$ MeV, $m_\mu = 106$ MeV.
- We use Lanczos, AMA, and zMobius techniques to speed up the computations.
- 65 configurations are used. They each are separated by 20 MD time units.

$$\left. \frac{g_\mu - 2}{2} \right|_{\text{cHLbL}} = (0.0926 \pm 0.0077) \times \left(\frac{\alpha}{\pi} \right)^3 = (11.60 \pm 0.96) \times 10^{-10} \quad (18)$$

$$\left. \frac{g_\mu - 2}{2} \right|_{\text{dHLbL}} = (-0.0498 \pm 0.0064) \times \left(\frac{\alpha}{\pi} \right)^3 = (-6.25 \pm 0.80) \times 10^{-10} \quad (19)$$

$$\left. \frac{g_\mu - 2}{2} \right|_{\text{HLbL}} = (0.0427 \pm 0.0108) \times \left(\frac{\alpha}{\pi} \right)^3 = (5.35 \pm 1.35) \times 10^{-10} \quad (20)$$

This is slightly partial quenched calculation performed on the 139 MeV pion mass ensemble.



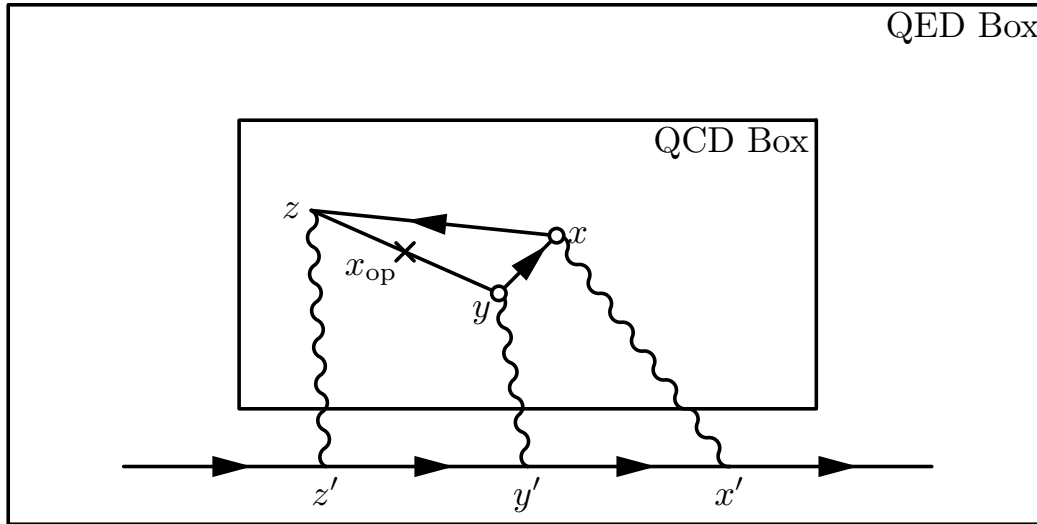
- Left: connected diagrams contribution. Right: leading disconnected diagrams contribution.
- $48^3 \times 96$ lattice, with $a^{-1} = 1.73$ GeV, $m_\pi = 139$ MeV, $m_\mu = 106$ MeV.
- $64^3 \times 128$ lattice, with $a^{-1} = 2.36$ GeV, $m_\pi = 135$ MeV, $m_\mu = 106$ MeV.

- Introduction
- Method
- Simulation
- **Infinite volume QED box**
- Summary

$$\mathcal{F}_\nu^C(x, y, z, x_{\text{op}}) = (-ie)^6 \mathcal{G}_{\rho, \sigma, \kappa}(x, y, z) \mathcal{H}_{\rho, \sigma, \kappa, \nu}^C(x, y, z, x_{\text{op}})$$

The QED part, $\mathcal{G}_{\rho, \sigma, \kappa}(x, y, z)$ can be evaluated in infinite volume QED box.

The QCD part, $\mathcal{H}_{\rho, \sigma, \kappa, \nu}^C(x, y, z, x_{\text{op}})$ can be evaluated in a finite volume QCD box.



$$i^3 \mathcal{G}_{\rho, \sigma, \kappa}(x, y, z) = \mathfrak{G}_{\rho, \sigma, \kappa}(x, y, z) + \mathfrak{G}_{\sigma, \kappa, \rho}(y, z, x) + \text{other 4 permutations.} \quad (21)$$

$$\begin{aligned} \mathfrak{G}_{\rho, \sigma, \kappa}(x, y, z) = & e^{m_\mu(t_{\text{snk}} - t_{\text{src}})} \sum_{x', y', z'} G_{\rho, \rho'}(x, x') G_{\sigma, \sigma'}(y, y') G_{\kappa, \kappa'}(z, z') \\ & \times \sum_{\vec{x}_{\text{snk}}, \vec{x}_{\text{src}}} S_\mu(x_{\text{snk}}, x') i\gamma_\rho S_\mu(x', y') i\gamma_\sigma S_\mu(y', z') i\gamma_\kappa S_\mu(z', x_{\text{src}}) \end{aligned} \quad (22)$$

How to evaluate $\mathfrak{G}_{\rho,\sigma,\kappa}(x, y, z)$? arXiv:1705.01067.

First, we need to regularize the infrared divergence in $\mathfrak{G}_{\rho,\sigma,\kappa}(x, y, z)$.

$$\mathfrak{G}_{\rho,\sigma,\kappa}(x, y, z) = \frac{1 + \gamma_0}{2} [(a_{\rho,\sigma,\kappa}(x, y, z))_k \Sigma_k + i b_{\rho,\sigma,\kappa}(x, y, z)] \frac{1 + \gamma_0}{2} \quad (23)$$

where $a_{\rho,\sigma,\kappa}(x, y, z)$ and $b_{\rho,\sigma,\kappa}(x, y, z)$ are real functions.

$$\mathfrak{G}_{\rho,\sigma,\kappa}^{(1)}(x, y, z) = \frac{1}{2} \mathfrak{G}_{\rho,\sigma,\kappa}(x, y, z) + \frac{1}{2} [\mathfrak{G}_{\kappa,\sigma,\rho}(z, y, x)]^\dagger \quad (24)$$

It turned out that $\mathfrak{G}_{\rho,\sigma,\kappa}^{(1)}(x, y, z)$ is infrared finite.

$$\begin{aligned} \mathfrak{G}_{\rho,\sigma,\kappa}^{(1)}(x, y, z) &= \frac{\gamma_0 + 1}{2} i \gamma_\sigma (\partial'_\zeta + \gamma_0 + 1) i \gamma_\kappa (\partial'_\xi + \gamma_0 + 1) i \gamma_\rho \frac{\gamma_0 + 1}{2} \\ &\times \int \frac{d^4 \eta}{4 \pi^2} \frac{f(\eta - y + \zeta) f(x - \eta + \xi) - f(y - \eta + \zeta) f(\eta - x + \xi)}{2(\eta - z)^2} \Big|_{\xi=\zeta=0} \end{aligned} \quad (25)$$

$$f(x) = f(|x|, x_t/|x|) = \frac{1}{8\pi^2} \int_0^1 dy e^{-yx_t} K_0(y|x|) \quad (26)$$

The 4 dimensional integral is calculated numerically with the CUBA library cubature rules.

Eventually, we need to compute

$$\sum_{x,y,z} \mathfrak{G}_{\rho,\sigma,\kappa}(x, y, z) \mathcal{H}_{\rho,\sigma,\kappa,\nu}^C(x, y, z, x_{\text{op}}) \quad (27)$$

$\mathcal{H}_{\rho,\sigma,\kappa,\nu}^C(x, y, z, x_{\text{op}})$ satisfies current conservation condition, which implies:

$$\sum_x \mathcal{H}_{\rho,\sigma,\kappa,\nu}^C(x, y, z, x_{\text{op}}) = 0 \quad (28)$$

$$\sum_z \mathcal{H}_{\rho,\sigma,\kappa,\nu}^C(x, y, z, x_{\text{op}}) = 0 \quad (29)$$

So, we have some freedom in changing $\mathfrak{G}_{\rho,\sigma,\kappa}(x, y, z)$. One choice we find particularly helpful is:

$$\mathfrak{G}_{\rho,\sigma,\kappa}^{(2)}(x, y, z) = \mathfrak{G}_{\rho,\sigma,\kappa}^{(1)}(x, y, z) - \mathfrak{G}_{\rho,\sigma,\kappa}^{(1)}(y, y, z) - \mathfrak{G}_{\rho,\sigma,\kappa}^{(1)}(x, y, y) + \mathfrak{G}_{\rho,\sigma,\kappa}^{(1)}(y, y, y)$$

Consider a vector field $J_\rho(x)$. It satisfies two conditions:

- $\partial_\rho J_\rho(x) = 0$.
- $J_\rho(x) = 0$ if $|x|$ is large.

We can conclude (the result is a little bit unexpected, but actually correct):

$$\int d^4x J_\rho(x) = 0 \quad (30)$$

In three dimension, this result have a consequence which is well-known.

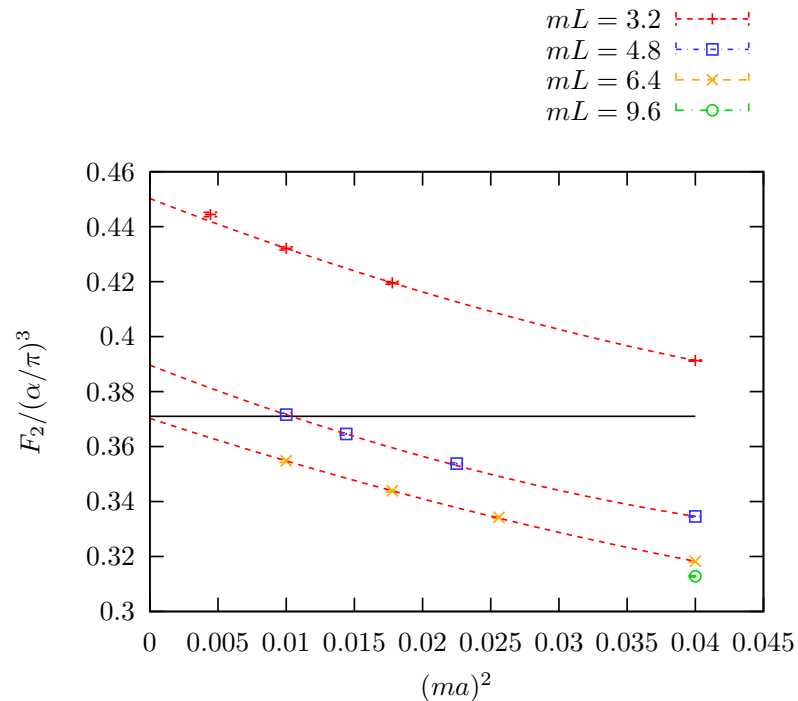
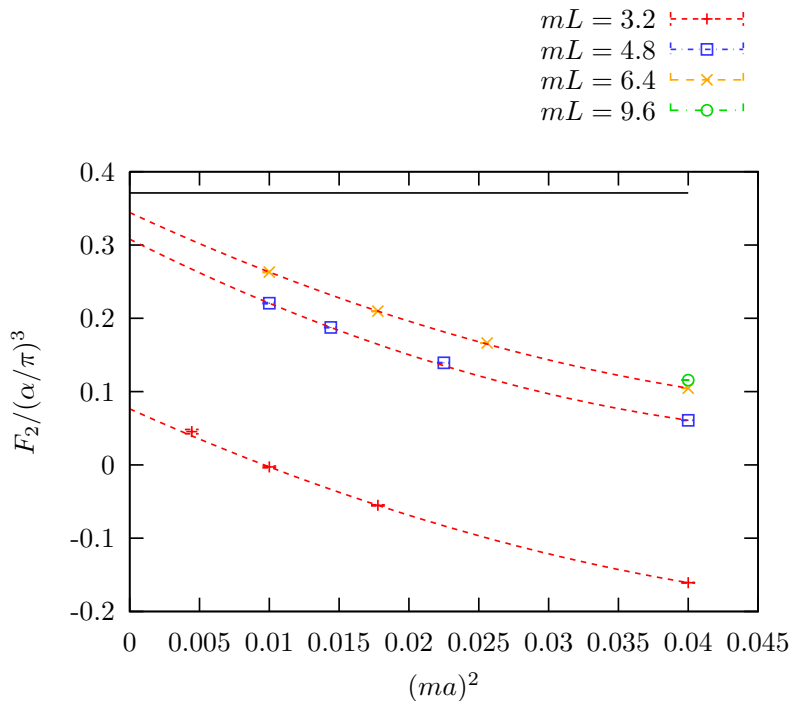
Consider a finite size system with stationary current. We then have

- $\vec{\nabla} \cdot \vec{j}(\vec{x}) = 0$, because of current conservation.
- $\vec{j}(\vec{x}) = 0$ if $|\vec{x}|$ large, because the system if of finite size.

Within a constant external magnetic field \vec{B} , the total magnetic force should be

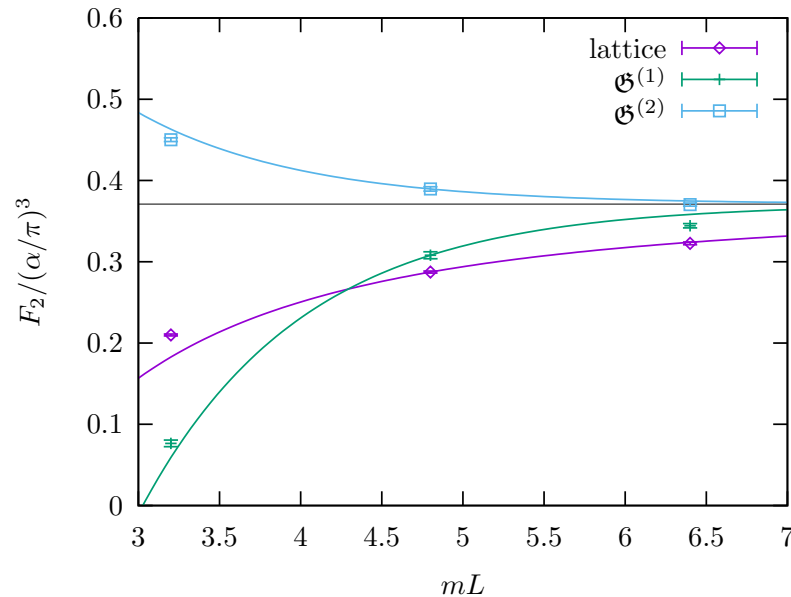
$$\int [\vec{j}(\vec{x}) \times \vec{B}] d^3x = \left[\int \vec{j}(\vec{x}) d^3x \right] \times \vec{B} = 0 \quad (31)$$

- Compare the two $\mathcal{G}_{\rho,\sigma,\kappa}(x, y, z)$ in **pure QED computation**.



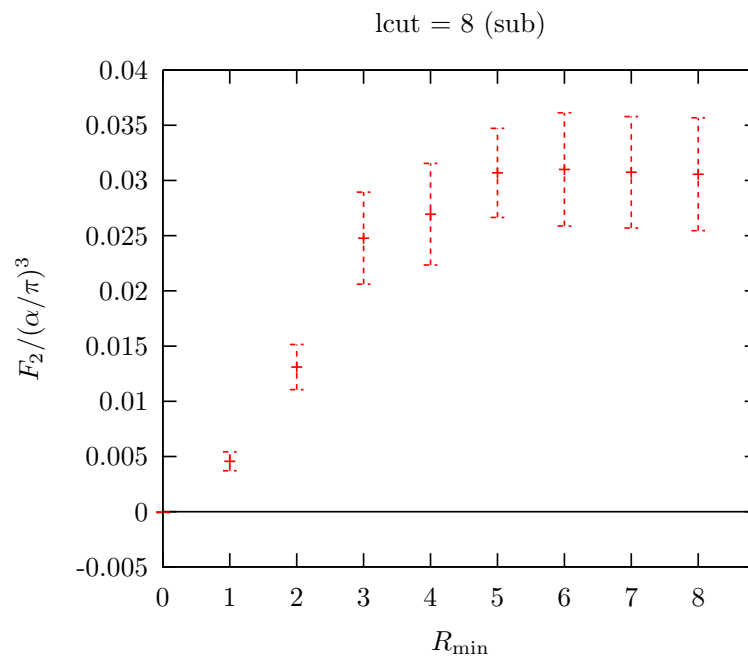
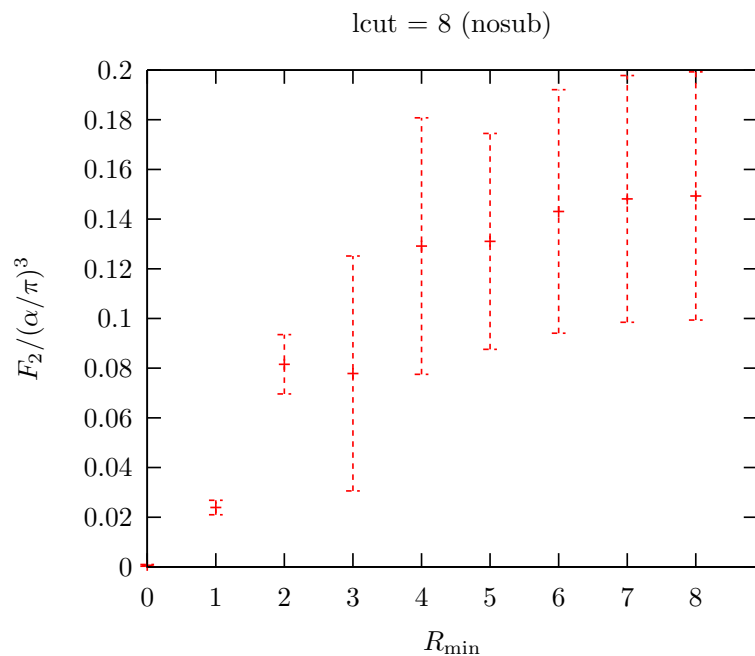
- Left: $\mathcal{G}^{(1)}$.
- Right: $\mathcal{G}^{(2)}$. Subtraction is performed on $\mathcal{G}^{(1)}$.
- Notice the vertical scales in the two plots are different.

- Compare the finite volume effects in different approaches in **pure QED computation**,



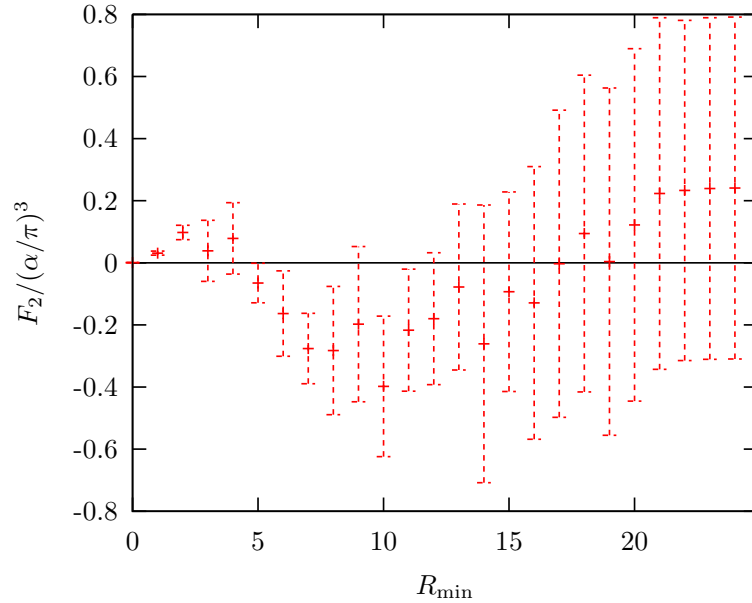
- Lattice: $\mathcal{O}(1/L^2)$ finite volume effect, because the photons are emitted from a conserved loop. Phys.Rev. D93 (2016) 1, 014503.
- $\mathcal{G}^{(1)}$: $\mathcal{O}(e^{-mL})$ finite volume effect. Everything except the four-point-correlation function is evaluated in infinite volume. arXiv:1705.01067.
- $\mathcal{G}^{(2)}$: smaller $\mathcal{O}(e^{-mL})$ finite volume effect. arXiv:1705.01067.

- Only connected diagram, 1 configuration. Errors are estimated by perform 8 “independent” measurements on the same configurations.
- Physical pion mass and $a = 0.2 \text{ fm}$. Dislocation Suppressing Determinant Ratio (DSDR) to suppress the sampling of topological sectors at this coarse lattice spacing. For light hadronic variables, scaling errors are about a 1% effect.

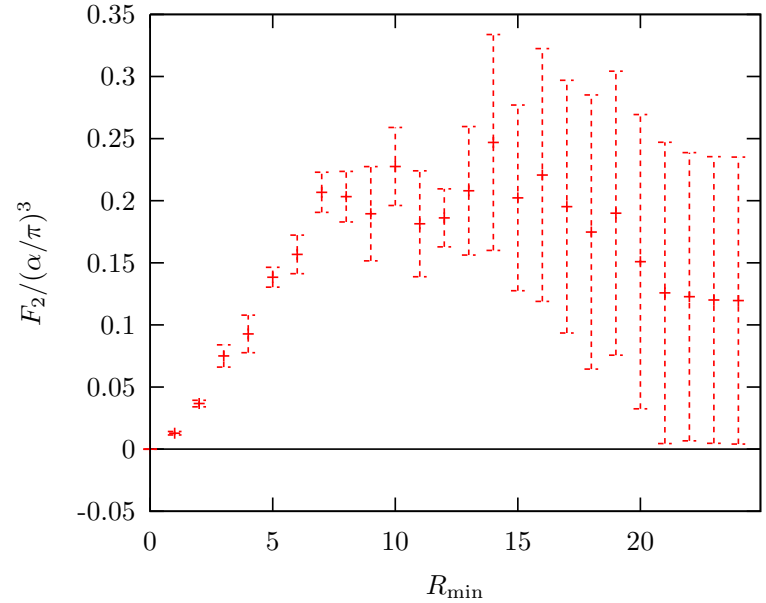


- nosub $\mathcal{G}^{(1)}$ v.s sub $\mathcal{G}^{(2)}$.
- $\max(|x - y|, |x - z|, |y - z|) \leq \text{lcut} = 8$. $\min(|x - y|, |x - z|, |y - z|) \leq R_{\min}$

lcut = 24 (nosub)



lcut = 24 (sub)



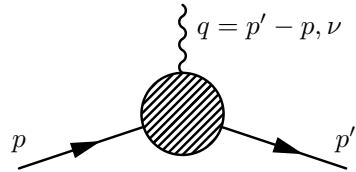
- nosub $\mathcal{G}^{(1)}$ v.s sub $\mathcal{G}^{(2)}$.
- $\max(|x - y|, |x - z|, |y - z|) \leq l_{\text{cut}} = 24$. $\min(|x - y|, |x - z|, |y - z|) \leq R_{\min}$

- Introduction
- Method
- Simulation
- Infinite volume QED box
- **Summary**

Recent model $a_\mu^{\text{HLbL}} \times 10^{10} = 10.3 \pm 2.9$. [arXiv:1705.00263](#).

- In a finite $(5.5 \text{ fm})^3$ box with inverse lattice spacing $1/a = 1.73 \text{ GeV}$, we obtained $a_\mu^{\text{HLbL}} \times 10^{10} = 5.35 \pm 1.35$, except for some subleading disconnected diagrams.
- We expect rather large **finite volume errors** and **discretization errors**.
- Using the **infinite volume QED** weighting function to eliminate the power-law suppressed finite volume effects.
- Repeat the calculation with a **larger coarse lattice** to study the exponentially suppressed finite volume effects.
- Repeat the calculation with the $1/a = 2.36 \text{ GeV}$ **fine lattice** to reduce the discretization errors.

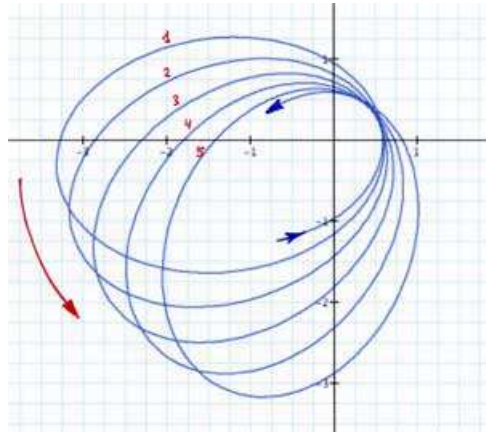
Thank You!



		$a_\mu \times 10^{10}$	Reference
Experiment		11659208.9 ± 6.3	E821, $g - 2$ Collab. 2006
Standard Model	???	11659182.8 ± 5.0	Particle Data Group, 2014
		26.1 ± 8.1	

Future is hard to predict, let's think of something similar in the history.

Precession of the perihelion of Mercury (in unit of arcsec/Julian century)



	Precession	Reference
Experiment	574.10 ± 0.65	G. M. Clemence 1947
Newton's Law	531.63 ± 0.69	G. M. Clemence 1947
???	42.47 ± 0.95	